Biogeosciences Discuss., 9, 19199–19243, 2012
www.biogeosciences-discuss.net/9/19199/2012/
doi:10.5194/bgd-9-19199-2012

Biogeosciences Discussions

Assessing the role of dust deposition on phytoplankton ecophysiology and succession in a low-nutrient low-chlorophyll ecosystem: a mesocosm experiment in the Mediterranean Sea

V. Giovagnetti[1], C. Brunet[1], F. Conversano[1], F. Tramontano[1], I. Obernosterer[2,3], C. Ridame[4], and C. Guieu[5,6]

[1]Stazione Zoologica Anton Dohrn, Villa Comunale, 80121, Naples, Italy
[2]Université Pierre et Marie Curie-Paris 6, UMR 7621, LOMIC, Observatoire Océanologique, F-66650 Banyuls/Mer, France
[3]CNRS, UMR 7621, LOMIC, Observatoire Océanologique, 66650 Banyuls/Mer, France
[4]Laboratoire d'Océanographie et du Climat: Expérimentations et Approches Numériques (LOCEAN), CNRS-Université Paris VI, Campus Jussieu, Paris, France
[5]Laboratoire d'Océanographie de Villefranche/Mer, CNRS-INSU, UMR7093, Observatoire Océanologique, 06230, Villefranche/Mer, France
[6]Université Pierre et Marie Curie-Paris 6, UMR 7093, LOV, Observatoire Océanologique, 06230, Villefranche/Mer, France

Received: 30 November 2012 – Accepted: 5 December 2012 – Published: 21 December 2012

Correspondence to: C. Brunet (christophe.brunet@szn.it)

Published by Copernicus Publications on behalf of the European Geosciences Union.

BGD
9, 19199–19243, 2012

Abstract

In this study, we investigate the phytoplankton community response, with emphasis on ecophysiology and succession, after two experimental additions of Saharan dust in the surface layer of a low-nutrient low-chlorophyll ecosystem in the Mediterranean Sea. Three mesocosms were amended with evapocondensed dust to simulate realistic Saharan dust events while three additional mesocosms were kept unamended and served as controls. Experiments consisted in two consecutive dust additions and samples were daily collected at different depths (−0.1, −5 and −10 m) during one week, starting before each addition occurred. Data concerning HPLC pigment analysis on two size classes (< 3 and > 3 µm), electron transport rate (ETR) versus irradiance curves, non-photochemical fluorescence quenching (NPQ) and phytoplankton cell abundance (measured by flow cytometry), are presented and discussed in this paper. Results show that picophytoplankton mainly respond to the first dust addition, while the second addition leads to an increase of both pico- and nano-/microphytoplankton. Ecophysiological changes in the phytoplankton community are revealed, and an increase in NPQ development, as well as in pigment concentration per cell, follows the dust additions. ETR does not show large variations between dust-amended and control conditions, while biomass increases in response to the dust additions. Furthermore, the biomass increase observed during this mesocosm experiment allows us to attempt a quantitative assessment and parameterization of the onset of a phytoplankton bloom in a nutrient-limited ecosystem.

These results are discussed focusing on the adaptation of picophytoplankton to such a nutrient-limited mixed layer system, as well as on size-dependent competition ability in phytoplankton.

BGD

9, 19199–19243, 2012

1 Introduction

Nutrient limitation is a general feature of the major part of pelagic ecosystems (oligotrophic areas), strongly affecting phytoplankton life dynamics, in term of biomass, functional diversity, cell size dominance and taxonomic composition. Such types of ecosystem are generally far from any coastal influence, and are usually characterized by high light at the surface layer and a deep euphotic zone (Dugdale and Goering, 1967; Kirk, 1994).

Low nutrient concentration and high light pressure largely influence phytoplankton productivity and growth, selecting species that are adapted to thrive in such abiotic conditions. For few decades, strong efforts have been devoted to the investigation of the deep chlorophyll maximum (DCM), an oceanographic phenomenon widespread in the oligotrophic pelagic ecosystems, with several studies being focused on DCM formation and maintenance, as well as the biological and ecological features of its phytoplankton community (e.g. Cullen, 1982; Gould, 1987; Pérez et al., 2006).

Bio-oceanographers have often paid limited attention to the phytoplankton community growing in the surface layer (Marañón, 2005; Davey et al., 2008; Moore et al., 2008), being usually characterized by a low biomass and production also related to the dominance of small-sized cells (mainly prokaryotic species), decreasing its ecological and biogeochemical relevance when compared to DCM or coastal ecosystems. Indeed, during oceanographic cruises, the first ten metres of the pelagic water realm are scarcely sampled – in most cases water samples are taken at only one depth within this portion of the water column – causing a paucity of data by which defining the biotic and abiotic properties of this system. However, since the direct contact with the atmosphere, a feature that can strongly influence temperature, light and nutrient availability of the water mass, the surface layer of pelagic ecosystems might be sensibly affected by the ongoing climate change (Marinov et al., 2010). Due to the important amount of biogeochemically relevant elements contained in the continental crust (Wedepohl, 1995), the atmosphere is vehicle of a significant transport of many

BGD
9, 19199–19243, 2012

natural and anthropogenic micro- and macronutrients, from continents to the surface of the oceans (Duce et al., 1991; Paerl et al., 1999). Moreover, the impact of such atmospheric inputs of nutrients on the functioning and biological cycles of the aquatic ecosystem becomes particularly strong when oligotrophic oceanic regions and semi-enclosed basins (such as the Mediterranean Sea) are taken into account (Guerzoni et al., 1999; Ridame and Guieu, 2002).

Despite great interest has been dedicated upon the effect of atmospheric forcing (especially iron) on "high-nutrient low-chlorophyll" (HNLC) open ocean regions (e.g. Boyd et al., 2007; Blain et al., 2008), several studies, based on microcosm experiments, have been also performed to better understand the influence exerted by atmospheric inputs of nutrients on the functioning and productivity in "low-nutrient low-chlorophyll" (LNLC) environments, either in the Atlantic Ocean (Blain et al., 2004; Mills et al., 2004; Moore et al., 2008; Marañón et al., 2010), Pacific Ocean (Law et al., 2011), and Mediterranean Sea (Pulido-Villena et al., 2008; Wagener et al., 2010).

The Mediterranean Sea might receive high rates of aeolian dust, of both natural (Saharan) and anthropogenic origin, over wide areas (e.g. Guerzoni et al., 1999; Ridame and Guieu, 2002; Pulido-Villena et al., 2008). These atmospheric inputs probably represent the main source of external nutrients reaching offshore surface mixed layers (Bartoli et al., 2005; Guieu et al., 2010a). In the western Mediterranean oligotrophic areas, significant amounts of iron (Bonnet and Guieu, 2008) and phosphorus (Ridame and Guieu, 2002) can be delivered to the surface waters through Saharan dust pulses (Bergametti et al., 1992; Guieu et al., 2002), and significant changes in the autotrophic (and heterotrophic) community structure have been evidenced (Bonnet et al., 2005; Pulido-Villena et al., 2008) in relation to Saharan dust additions.

In oligotrophic waters, the greatest part of the algal community is formed by tiny cells belonging to the size-class of picophytoplankton ($< 3\,\mu m$), which have peculiar characteristics with respect to their ecology and biology (Raven, 1998; Raven et al., 2005; Worden and Not, 2008; Finkel et al., 2010). The low sinking rate and package effect, as well as the high diversity of photosynthetic pigments and efficient capacity

BGD
9, 19199–19243, 2012

of light utilization (Raven, 1998; Raven et al., 2005), represent some of the advantageous hallmarks of picophytoplankton. Their cell size-related low diffusion boundary layer and large surface area per unit volume explain the dominance of small phytoplankters in oligotrophic waters, since their greater capacity and efficiency in resources (i.e. nutrients and light) acquisition/use for cell growth and maintenance, than bigger ones (Raven, 1998). The number of studies tackling the diversity and ecology of picophytoplankton has been recently grown (Le Gall et al., 2008; Vaulot et al., 2008; Finkel et al., 2010), together with the amount of works focused on the investigation of the ecophysiology of picoeukaryotes (Dimier et al., 2007, 2009a, 2009b; Six et al., 2008, 2009; Giovagnetti et al., 2010, 2012).

Among the picophytoplankton, oxygenic phototrophic marine cyanobacteria belonging to the genera *Synechococcus* (Waterbury et al., 1979) and *Prochlorococcus* (Chisholm et al., 1988, 1992) often appear to be dominant in oligotrophic waters, co-occurring with changing relative proportions (Veldhuis and Kraay, 1990), since their different types of adaptation to biogeochemical conditions (Partensky et al., 1999). In association with picoeukaryotes, both genera might be considered the major contributors of biomass and primary production in oligotrophic environments (Morel et al., 1993; Partensky et al., 1999). Picophytoplankton relevant contribution to total phytoplankton biomass and production is also well known in the Mediterranean Sea (Magazzù and Decembri, 1995; Casotti et al., 2003; Brunet et al., 2006, 2008). Despite different studies have recently revealed the high specific diversity and ubiquity of picoeukaryotes (Moon-van der Staay et al., 2001; Díez et al., 2001; Not et al., 2002, 2005), few in field studies have performed pigment in fractionated samples coupled with flow cytometry analysis, to deeply investigate the ecology of picoeukaryotes (Brunet et al., 2006, 2008; Not et al., 2005).

By applying a mesocosm approach in the framework of the DUNE project (a DUst experiment in a low-Nutrient, low-chlorophyll Ecosystem; see Guieu et al., 2010b), this study (DUNE-2) aimed at addressing the following specific questions: which is the size class of phytoplankton better able to exploit the new nutrient resource coming from the

BGD
9, 19199–19243, 2012

dust additions, in terms of growth capacity and competition dynamics? Which chemotaxomic group(s) is (are) able to succeed competition? And lastly, are new nutrient inputs affecting the ecophysiological properties of the phytoplankton community, and how?

Mesocosm deployment provides a unique and powerful tool to study the response to chemical forcing (such as atmospheric deposition) of the phytoplankton community over time, by preventing the horizontal advection and transport of the water mass, while enabling to carefully investigate the temporal changes of the biological properties of interest.

The mesocosm experiment DUNE-2 was conducted in the Elbo Bay, a coastal LNLC area of the Mediterranean Sea, within the Natural Preservation Area of Scandola, and the approach consisted of two consecutive dust additions onto large clean mesocosms (see the introductory paper by Guieu et al., 2012). In this paper, we report data from daily sampling in six mesocosms concerning pigment content (HPLC and ChemTax analysis) of two size classes (< 3 and $> 3\,\mu m$), electron transport rate (ETR) versus irradiance (I) curves, non-photochemical fluorescence quenching (NPQ), phytoplankton cell concentration through flow cytometry, together with nutrient analysis.

2 Materials and methods

2.1 Experimental design and sampling strategy

A dust deposition experiment onto large clean mesocosms was conducted in June–July 2010 in a coastal area of the Corsica island (NW Mediterranean Sea), the Elbo Bay (Scandola Marine preservation area, 42° 37′ N, 8° 55′ E), which is representative of typical marine oligotrophic conditions (Guieu et al., 2010b). Ecological properties of the area at the time of sampling corresponded to the transition period between spring and summer conditions, with low nutrient and low chlorophyll concentrations, coupled with the onset of the thermal stratification (Guieu et al., 2012).

BGD
9, 19199–19243, 2012

Two dust additions (duration seven days each, 26 June–2 July 2010, and 3–9 July 2010) were performed (all information and methodologies are reported in Guieu et al., 2012). Three mesocosms (named DUST Mesocosms: DM1, DM2, and DM3) were amended with 41.5 g of evapocondensed dust each, while three mesocosms, with no addition of dust, were used as controls (CONTROL Mesocosms: CM1, CM2 and CM3). Moreover, a station, outside the mesocosms was used as control for eventual biases due to the structure of the mesocosms (named "outside"). Samples were daily collected at three depths (−0.1, −5 and −10 m), at the same hour of the morning, with the only exception of the outside station, where sampling frequency was set to 48 h.

In this study we report data on photosynthetic parameters (retrieved from ETR-I curves) and NPQ (measured by Phyto-PAM fluorometer), photosynthetic and photoprotective pigments (measured by HPLC analysis), and phytoplankton cell abundance (measured by flow cytometry).

2.2 Pigment and ChemTax analysis

Soon after sampling, samples were kept in the dark while carried to the field laboratory, and for each one of them, three litres of seawater were filtered onto polycarbonate filters of 3 µm pore size (Merck Millipore, Darmstadt, Germany) and one litre of the filtrate was then poured onto polycarbonate filters of 0.2 µm. Both filters were rapidly stored in liquid nitrogen. In the laboratory (Stazione Zoologica Anton Dohrn, Naples), frozen filters were mechanically grinded in 100 % methanol and the pigment extract was injected in a Hewlett Packard series 1100 HPLC (Hewlett-Packard, Kennett Square, PA, USA) with a C_8 BDS 3 µm Hypersil, IP column (Thermo Fisher Scientific, Waltham, MA, USA). The procedure was the same as described in Dimier et al. (2009a). The mobile phase was composed of two solvent mixtures: methanol, aqueous ammonium acetate (70 : 30) and methanol. Pigments were detected spectrophotometrically at 440 nm using a Hewlett Packard photodiode array detector model DAD series 1100. Fluorescent pigments were detected in a Hewlett Packard standard FLD cell series 1100 with excitation and emission wavelengths set at 407 nm and 665 nm, respectively. Determination

BGD
9, 19199–19243, 2012

and quantification of pigments was performed by using pigment standards from the Danish Hydraulic Institute (DHI) Water & Environment (Hørsholm, Denmark).

The contribution of each phytoplankton group to total phytoplankton biomass (chlorophyll [Chl] *a*) was estimated by using the ChemTax program with input ratios slightly modified from Rodriguez et al. (2006) and Not et al. (2007).

2.3 Active Chl *a* fluorescence and photosynthetic efficiency measurements

Measurements of non-photochemical fluorescence quenching (NPQ) and electron transport rate (ETR) versus irradiance (*I*) curves were performed daily on freshly collected samples, with a Phyto-PAM fluorometer (Heinz Walz GmbH, Effeltrich, Germany).

Since the low phytoplankton cell abundance in seawater, samples were concentrated for PAM measurements. Fifty millilitres of seawater were gently filtered onto polycarbonate filters (Merck Millipore, Darmstadt, Germany) of 0.45 µm pore size. Filters were then moistened and cells were immediately resuspended in five millilitres of filtered seawater (< 0.2 µm). All these operations were done under very low light condition. This procedure was successfully tested in laboratory on coastal mesotrophic samples (Gulf of Naples, Mediterranean Sea) and on diatom cultures with different cell concentrations, before applying it to the field experiment, in order to check if the concentration procedure would have induced any stress, thus modifying the results. Since no differences were obtained between concentrated and non-concentrated samples, we applied this method during the mesocosm experiment.

After fifteen minutes in dark, an aliquot of two millilitres was used for measurements of ETR-I curves, and then another two millilitres aliquot to estimate NPQ.

NPQ was quantified by the Stern–Volmer expression:

$$NPQ = (Fm/Fm') - 1 \quad (1)$$

where Fm and Fm′ are the maximum fluorescence values from dark- and light-exposed samples, respectively. Fm and Fm′ were measured after a saturating pulse of red light

BGD
9, 19199–19243, 2012

(2400 µmol photons $m^{-2} s^{-1}$, lasting 450 ms), causing a complete reduction of the photosystem (PS) II acceptor pool.

ETR-I curves were determined applying 10 increasing irradiances (I, from 1 to 1500 µmol photons $m^{-2} s^{-1}$ for 2 min each).

The relative electron transport rate ($_{rel}ETR_{max}$, expressed in µmol $e^- m^{-2} s^{-1}$) was calculated according to Hofstraat et al. (1994) and Schreiber et al. (1994):

$$_{rel}ETR_{max} = (Fv'/Fm') \cdot I \cdot 0.5 \quad (2)$$

where, I is the incident irradiance (expressed in µmol photons $m^{-2} s^{-1}$). A factor of 0.5 was applied to correct for the partitioning of photons between PSI and PSII, assuming that excitation energy is evenly distributed between the two photosystems.

ETR-I curves were fitted with the equation of Eilers and Peeters (Eilers and Peeters, 1988) to estimate the photosynthetic parameters $_{rel}\alpha^B$, Ek and $_{rel}ETR_{max}$.

2.4 Flow cytometry

For the enumeration of autotrophic prokaryotic and eukaryotic cells by flow cytometry, subsamples (four millilitres) were fixed with formaldehyde (2 % final conc.), and incubated for 30 min at 4 °C, then quick-frozen in liquid nitrogen and stored at −80 °C until analysis. Counts were performed on a FACS-Calibur flow cytometer (Becton Dickinson, San Jose, CA, USA) equipped with a 488 nm wavelength, 15 mW Argon laser. Separation of different autotrophic populations was based on their scattering and fluorescence signals according to Marie et al. (2000). *Synechococcus* spp. was discriminated by its strong orange fluorescence (585 ± 21 nm), and pico- and nanoeukaryotes were discriminated by their scatter signals of red fluorescence (> 670 nm). The coefficient of variation is generally < 5 % (Agogué et al., 2004).

BGD
9, 19199–19243, 2012

2.5 Statistical analysis

Student's t-test and multiple regressions conducted on the entire data set between the measured Chl *a* concentration in the two size classes and the Chl *a* concentration of the specific groups (ChemTax analysis), as well as between cellular abundances (flow cytometry) and Chl *a*-group specific abundance values (ChemTax analysis), were performed by using the program Statistica (StatSoft, OK, USA).

The integration of the data sets concerning pigments (> 3 µm) and nanophytoplankton cellular abundance (flow cytometry) was performed based on the assumption of a very low microphytoplanktonic biomass (so their negligible contribution to total Chl *a*) in relation with the severe oligotrophic field conditions, and in agreement with the very low biomass of large-sized *Bacillariophyceae* (ChemTax analysis; see result section).

3 Results

3.1 Evolution of the abiotic conditions during the experiment

During the entire experiment, light was high, reaching peaks of $\sim 900\,\mu mol\,photons\,m^{-2}\,s^{-1}$ at the subsurface (see data in Guieu et al., 2012). Air and seawater temperature increased over the experiment time, leading to the switch from a homogeneous to a stratified water mass structure (Guieu et al., 2012).

Before the first dust addition was performed, the initial concentration of nutrients was undetectable (nitrate and nitrite) or low (phosphate), while the concentration of nitrate (Ridame et al., 2012) and phosphate (Pulido-Villena et al., 2012) increased soon after the dust additions. The concentration of the dissolved iron was quite high possibly due to iron inputs related to particle runoff of surrounding lands, and decreased after the first dust addition (especially in the DUST Mesocosms), while significantly increasing after the second addition in the DUST Mesocosms and remaining stable in the CONTROL ones (Wuttig et al., 2012).

BGD
9, 19199–19243, 2012

By contrast, the concentration of silica was higher than the other macronutrients and remained quite stable after the dust additions (Guieu et al., 2012).

3.2 Phytoplankton biomass and community diversity

Once verified that no significant difference occurred between mesocosm triplicates both for DUST and CONTROL conditions ($p > 0.05$, $n = 112$), mean data of the three mesocosms-replicates are presented.

In DUST Mesocosms (hereafter called DM), the first dust addition induced a picophytoplankton biomass increase (Chl $a_{<3}$; Fig. 1a), from ~ 0.03 to $\sim 0.06\,\mu g\,Chl\,a_{<3}\,L^{-1}$, all over the three depths, reaching a maximal value of $0.056 \pm 0.018\,\mu g\,Chl\,a_{<3}\,L^{-1}$ at the surface, five days after the first dust addition (Fig. 1a). In CONTROL Mesocosms (hereafter called CM), the Chl $a_{<3}$ concentration was clearly lower than in DM, ranging from ~ 0.02 to $\sim 0.03\,\mu g\,Chl\,a_{<3}\,L^{-1}$ (Fig. 1b). The response of the nano- and microphytoplanktonic component (Chl $a_{>3}$) to the first dust addition was less strong than the picophytoplanktonic one, with Chl $a_{>3}$ concentration slightly increasing from ~ 0.014 to $\sim 0.020\,\mu g\,Chl\,a_{>3}\,L^{-1}$ (Fig. 1c).

After the second dust addition, the increase of Chl $a_{<3}$ biomass was strong (reaching $0.083 \pm 0.011\,\mu g\,Chl\,a_{<3}\,L^{-1}$), mainly at the surface, while decreasing with depth (Fig. 1a) probably as a result of thermal stratification. The increase in Chl $a_{>3}$ concentration was much more enhanced during the second dust addition (i.e. the day after the second dust addition) relative to the first one, all over the depth gradient, but especially at the surface (reaching $0.046 \pm 0.002\,\mu g\,Chl\,a_{>3}\,L^{-1}$; Fig. 1c).

The seasonal transition period, revealed by changes in temperature properties of the water mass from the middle of the experiment (2 July), might explain the increase in biomass found in CM both for Chl $a_{<3}$ and Chl $a_{>3}$ concentrations (Fig. 1b, d). Temperature effect on growth rate of phytoplankton is well-known (see Chen and Liu, 2010, and references therein).

BGD
9, 19199–19243, 2012

It can be highlighted that the delay of the nano- and microphytoplankton response relative to the picophytoplankton one, in relation to the variations of the water mass temperature (CM), agrees with the similar delay found after the dust additions (DM).

Picophytoplankton accounted for ~ 70 % of total phytoplankton biomass, in both DM and CM, remaining almost stable during the entire experiment, while decreasing to ~ 60 % after the second dust addition, only in DM (Fig. 1e, f).

Concerning the contribution of phytoplankton groups on the two size classes, we performed multiple regressions on the entire data set (i.e. samples taken soon before and after each dust addition) between the measured Chl *a* concentration of the two size classes and the Chl *a* concentration of the specific groups (retrieved from ChemTax analysis):

$$\text{Chl } a_{<3} = 0.04_{Prasinophyceae} + 0.107_{Dinophyceae} + 0.535_{Haptophyceae} + 0.270_{Pelagophyceae} + 0.566_{Cyanophyceae} + 0.058_{Bacillariophyceae} \quad (3)$$

$$\text{Chl } a_{>3} = 0.007_{Prasinophyceae} + 0.228_{Dinophyceae} + 0.310_{Haptophyceae} + 0.406_{Chlorophyceae} + 0.077_{Cyanophyceae} + 0.233_{Bacillariophyceae} \quad (4)$$

Picophytoplanktonic diversity (in terms of Chl $a_{<3}$ concentration) was mainly dominated by *Cyanophyceae*, *Haptophyceae* and *Pelagophyceae* ($n = 113$, $R^2 = 0.99$, $p < 0.001$), while *Chlorophyceae*, *Haptophyceae*, *Bacillariophyceae* and *Dinophyceae*, were the dominant groups for the nano- and microphytoplanktonic component ($n = 114$, $R^2 = 0.99$, $p < 0.001$).

Haptophyceae, *Cyanophyceae* and *Pelagophyceae* were the most represented picoplanktonic taxonomic groups, all responding to the dust additions (Fig. 2). Even if less abundant, *Prasinophyceae*, *Dinophyceae* and *Bacillariophyceae* were also present (data not shown).

Before the first dust addition, *Haptophyceae* were the main contributor to the Chl $a_{<3}$concentration, with an initial Chl $a_{<3}$concentration of ~ 0.014 µg Chl $a_{<3}$ L^{-1} (Fig. 2a, b). The biomass of this group increased (up to 0.028 ± 0.003 µg Chl $a_{<3}$ L^{-1};

BGD
9, 19199–19243, 2012

Fig. 2a) five days after the first dust addition, while it quickly responded to the second addition, reaching $0.039 \pm 0.005\,\mu g\,Chl\,a_{<3}\,L^{-1}$. In CM, the biomass values of *Haptophyceae* were lower than the DM ones, ranging between ~ 0.006 and $\sim 0.020\,\mu g\,Chl\,a_{<3}\,L^{-1}$ (Fig. 2b).

The initial Chl $a_{<3}$ concentration of *Cyanophyceae* ($0.010 \pm 0.004\,\mu g\,Chl\,a_{<3}\,L^{-1}$) increased at the surface in response to the first ($0.020 \pm 0.004\,\mu g\,Chl\,a_{<3}\,L^{-1}$) and second dust addition ($0.024 \pm 0.008\,\mu g\,Chl\,a_{<3}\,L^{-1}$; Fig. 2c). An increase in the biomass of *Cyanophyceae* can be noticed at the end of the experiment ($\sim 0.030\,\mu g\,Chl\,a_{<3}\,L^{-1}$; Fig. 2c). In CM, the biomass of *Cyanophyceae* ranged between ~ 0.003 and $\sim 0.012\,\mu g\,Chl\,a_{<3}\,L^{-1}$, with no peculiar trend over time (Fig. 2d).

The initial Chl $a_{<3}$ concentration of *Pelagophyceae* was $\sim 0.008\,\mu g\,Chl\,a_{<3}\,L^{-1}$ (Fig. 2e, f) and it increased especially at the surface, after the first ($0.015 \pm 0.003\,\mu g\,Chl\,a_{<3}\,L^{-1}$) and second dust addition ($0.016 \pm 0.002\,\mu g\,Chl\,a_{<3}\,L^{-1}$; Fig. 2e). In CM, the biomass of *Pelagophyceae* ranged between ~ 0.004 and $\sim 0.012\,\mu g\,Chl\,a_{<3}\,L^{-1}$, without any peculiar trend over time and depth gradients (Fig. 2f).

Haptophyceae, *Chlorophyceae* and *Bacillariophyceae* accounted for the large majority of the nano- and microphytoplankton biomass. Other nano- and microphytoplanktonic groups (e.g. *Prasinophyceae*, *Dinophyceae*) were also found, but with lower biomass (data not shown).

The biomass of nano- and micro-*Haptophyceae* (Chl $a_{>3}$ concentration) mainly increased after the second dust addition (from ~ 0.008 to $\sim 0.015\,\mu g\,Chl\,a_{>3}\,L^{-1}$), whereas only slightly increasing after the first addition (Fig. 3a). In CM, the biomass of *Haptophyceae* was lower than in DM, and relatively stable over time and depth gradients (Fig. 3b), with the only exception at the end of the experiment, since the slight biomass increase concomitant to the water column thermal stratification.

The biomass of *Bacillariophyceae* was very low and it slightly increased after the first dust addition from ~ 0.0009 to $\sim 0.0020\,\mu g\,Chl\,a_{>3}\,L^{-1}$, whereas their greatest

BGD
9, 19199–19243, 2012

increase was found five-six days after the second addition, especially below 5 m (0.0092 ± 0.004 µg Chl $a_{>3}$ L^{-1}; Fig. 3c). In CM, the biomass of *Bacillariophyceae* was low and followed the same increasing trend as described previously for the biomass of *Haptophyceae* (Fig. 3d).

Chlorophyceae were only present in DM (Fig. 3e), underlining a very strong nutrient limitation for their growth in the control conditions and their possible opportunistic strategy in response to nutrient supply (Fig. 3f). Their Chl $a_{>3}$ concentration doubled mainly at the surface (from ~ 0.007 to ~ 0.013 µg Chl $a_{>3}$ L^{-1}) just after the second dust addition took place (Fig. 3e).

3.3 Phytoplankton abundances by flow cytometry measurements

Synechococcus was the dominant picophytoplankton in terms of cellular abundance. In DM, *Synechococcus* cellular abundance remained almost stable (~ 20 000 cell mL^{-1}) after the first dust addition, while it strongly increased after the second addition, reaching a value of $41\,806 \pm 3965$ cell mL^{-1}, at the end of the experiment (Fig. 4a). It can be noticed that the maximal *Synechococcus* cellular abundance was found below the 5 m depth. In CM, *Synechococcus* cellular abundance was lower than in DM (Fig. 4b), increasing from the middle of the experiment, as the Chl $a_{<3}$ concentration did.

Prochlorococcus cellular abundance was very low, ranging between ~ 500 and ~ 2500 cell mL^{-1}, confirming the lack of detection of divinyl-chlorophyll *a* pigment by HPLC analysis. No significant changes occurred in relation to the dust additions (data not shown).

Picoeukaryotes represented the least abundant picophytoplanktonic component, with a cellular abundance ranging between ~ 70 and ~ 470 cell mL^{-1} (Fig. 4c, d), without being particularly affected by the dust additions.

The cellular abundance of nanophytoplankton increased soon after the second dust addition from ~ 500 to ~ 950 cell mL^{-1}, especially at the surface, reaching a maximal value of 1351 ± 306 cell mL^{-1} on the last day of the experiment (Fig. 4e). In CM, the nanophytoplankton cellular abundance was low (Fig. 4f) and increased over the three

BGD
9, 19199–19243, 2012

depths (from ~300 to ~600 cell mL^{-1}; Fig. 4f), starting from the middle of the experiment.

Multiple regressions were performed on the complete data set (i.e. samples taken soon before and after each dust addition) between cellular abundance and Chl *a*-group specific concentration values. For the picophytoplankton community, none of the tested multiple regressions was significant, probably suggesting a huge diversity in pigment content of the distinct groups alternating during the experiment.

For the nanophytoplankton community, the obtained result is presented in Eq. (5) ($n = 112$, $R^2 = 0.52$, $p < 0.001$):

$$\text{Nano Cell Abundance} = 0.322_{Dinophyceae} + 0.349_{Haptophyceae} + 0.203_{Chlorophyceae} + 0.267_{Bacillariophyceae} \quad (5)$$

The highest pigment contribution to cellular abundance was due to *Haptophyceae*, followed by *Dinophyceae*, *Bacillariophyceae* and lastly *Chlorophyceae*, a finding that might highlight the distinct Chl *a* cellular content among these groups, in relation to their different cell size.

By reporting pigment data per cellular abundance data, we are able to describe some specific physiological changes concerning the phytoplanktonic community.

The ratio between zeaxanthin (Zeax) and *Synechococcus* cellular abundance increased after the first dust addition (from ~0.5 to ~1.3 fg Zeax cell^{-1}), and after the second addition only at the surface (from ~0.6 to ~1 fg Zeax cell^{-1}, Fig. 5a). In CM, this ratio was lower than 0.7 fg Zeax cell^{-1} (Fig. 5b).

An almost two-fold increase in Chl $a_{<3}$ concentration per picophytoplankton cell (from ~1.5 to ~3 fg Chl $a_{<3}$ cell^{-1}) rapidly occurred after the first dust addition, mainly at the surface, suggesting a very fast physiological response of picophytoplankton to the input of new nutrients (Fig. 5c). This response lasted for some days before decreasing, and increased again after the second dust addition (~3 fg Chl $a_{<3}$ cell^{-1}). In CM, the Chl $a_{<3}$ concentration per picophytoplankton cell was lower than 2.0 fg Chl $a_{<3}$ cell^{-1} (Fig. 5d).

BGD
9, 19199–19243, 2012

Comparing with other studies (e.g. Brunet et al., 2006, 2008; Dimier et al., 2009a, b), the Chl *a* content per picophytoplankton cell was quite low, a result that might reflect the high contribution of *Synechococcus* cells in such community, in relation to the lower Chl *a* cellular content of *Synechococcus* relative to picoeukaryotes, as well as to the high light acclimation of cells inhabiting the surface water layer.

The ratio between Chl $a_{>3}$ concentration and the nanophytoplankton cellular abundance ranged from $\sim 20\,\mathrm{fg\,Chl}\,a_{>3}\,\mathrm{cell}^{-1}$ to a maximal value of $60 \pm 10\,\mathrm{fg\,Chl}\,a_{>3}\,\mathrm{cell}^{-1}$ (Fig. 5e), quickly increasing the day after each dust addition ($\sim 40\,\mathrm{fg\,Chl}\,a_{>3}\,\mathrm{cell}^{-1}$, and $\sim 48\,\mathrm{fg\,Chl}\,a_{>3}\,\mathrm{cell}^{-1}$, after the first and second dust addition, respectively; Fig. 5e). In CM, the Chl $a_{>3}$ cell^{-1} remained low, ranging between ~ 13 and $\sim 28\,\mathrm{fg\,Chl}\,a_{>3}\,\mathrm{cell}^{-1}$ (Fig. 5f).

3.4 Photosynthetic parameters and photoprotective responses

One of the most intriguing obtained results was the absence of response of the PAM-estimated photosynthetic parameters to the dust additions, relative to the control condition. The photosynthetic parameters, the relative electron transport rate ($_{\mathrm{rel}}\mathrm{ETR}_{\mathrm{max}}$), the quantum yield of electron transport ($_{\mathrm{rel}}\alpha^{\mathrm{B}}$) and the light saturation index (Ek), remained almost stable over time, and similar values were measured among dust and control mesocosms (Fig. 6). These results contrast with those of the primary production through isotopic (^{13}C) measurements (^{13}C PP; data available only at 5 m depth, Ridame et al., 2012). This result might be explained by the fact that a gross ($_{\mathrm{rel}}\mathrm{ETR}_{\mathrm{max}}$) and a net primary production measurement (^{13}C PP) are compared. By plotting together these two parameters, some insights on the different net production capacity and photosynthetic process regulation of the two phytoplankton size classes are gained (Fig. 7).

The two parameters $_{\mathrm{rel}}\mathrm{ETR}_{\mathrm{max}}$ and ^{13}C PP were not significantly correlated by pooling together all the data of control and dust mesocosms, or all the data only coming from dust mesocosms (data not shown). By separating the two dust additions, no

BGD
9, 19199–19243, 2012

significant correlation was found in the block of the data set of the first dust addition (Fig. 7a), whereas $_{rel}ETR_{max}$ and ^{13}C PP were significantly correlated when only the block of the data set of the second dust addition was analyzed ($R^2 = 0.26$, $p < 0.05$; Fig. 7b). Interestingly, a significant correlation was also found between the data of $_{rel}ETR_{max}$ and ^{13}C PP measured in control mesocosms ($R^2 = 0.30$, $p < 0.01$; Fig. 7c). Therefore, in undisturbed conditions (i.e. the stable oligotrophy of the studied area), picophytoplankton, which represent the main contributor to total Chl *a* biomass, seem to be strongly adapted (at the physiological level) to the abiotic conditions of such ecosystem, as revealed by the significant agreement between gross and net primary production evolution.

Physiological changes induced by new nutrient inputs were also appreciated at the photophysiological level. Pigments belonging to the diadinoxanthin (Dd) xanthophyll cycle responded to dust additions in both size classes, being slightly higher than the more stable values of control conditions, with the photoprotective pigment, diatoxanthin, often at the limit of the HPLC detection level, since the size-fractionation of samples for pigment analysis (data not shown).

An increase in non-photochemical fluorescence quenching (NPQ) occurred after the first dust addition, from a very low initial value of ~0.006 to ~0.28 (Fig. 8a). After the second dust addition, the NPQ development still increased, to a value of ~0.48 at the surface, probably in relation to the higher contribution of the nano- and microphytoplanktonic component to the community, than after the first addition (Fig. 8a). In CM, NPQ was lower than in DM (Fig. 8b), and increased at the end of the experiment, in relation with the slight nano- and microphytoplankton biomass augment.

3.5 Phytoplankton (biomass) increase versus nutrient conditions

In this section, we describe and try to identify, which are the main factors allowing the phytoplankton growth after the first and the second dust addition. To address such question, we present the daily variations calculated on mean values of the data measured at 0.1 and 5 m depths, being these two depths homogeneous, contrarily to the

BGD
9, 19199–19243, 2012

deepest one (i.e. 10 m), that was quite different than the two other sampling depths after the second dust addition.

To perform such analysis, we assume that the impact of grazing or cell death might be considered negligible, during the three days that we selected. The selection of these specific days was based on the phytoplankton biomass increase occurring just after the dust additions.

The increase in Chl *a* concentration per day ($\mu g\,Chl\,a\,L^{-1}\,d^{-1}$) for the two phytoplankton size classes and the relative decrease in nutrient concentration ($\mu g\,nutrient\,L^{-1}\,d^{-1}$), two and three days after the first dust addition, are reported in Table 1. Two days after the first dust addition, i.e. after one lag day, only the picophytoplankton was able to increase their Chl *a* biomass, mainly with an increase in *Cyanophyceae* (~ 77 %) and *Haptophyceae* (~ 23 %). Differently, three days after the first dust addition, an increase in the nano- and microphytoplankton biomass was found (Table 1). Comparing the biomass and nutrient variations two and three days after the dust addition, in order to reach the same daily biomass augment, the nano- and microphytoplankton would need similar [NO_3^-] and [PO_4^{3-}], but almost two-fold lower [SiO_2], and four-fold higher [DFe], than the picophytoplankton. A similar [NO_3^-] need for the two size classes of phytoplankton was quite unexpected. We can hypothesize that the nano- and microphytoplankton underwent nitrogen limitation when they began to respond to the first dust addition, since the available nitrate concentration was very low (~ 0.50 µM, i.e. almost four-fold lower than the value measured at the surface soon after the first dust addition; see Ridame et al., 2012).

The increase in Chl *a* concentration per day for the two size classes and the relative decrease in nutrients, one day after the second dust addition, are reported in Table 1. In this case, the response of the phytoplanktonic community was much stronger than the one after the first addition, with an almost three-fold higher Chl a_{Tot} increase ($0.0271\,\mu g\,Chl\,a_{Tot}\,L^{-1}\,d^{-1}$; Table 1), relative to the first addition ($0.0091\,\mu g\,Chl\,a_{Tot}\,L^{-1}\,d^{-1}$). During the second dust addition, a 48 % contribution to total biomass increase was due to nano- and microphytoplankton (Table 1), i.e. a greater

BGD
9, 19199–19243, 2012

contribution relative to their percentage after the first dust addition (35 %; data not shown), consistently with the greater use of [NO_3^-] and [PO_4^{3-}] (Table 1), which agrees with the nutrient repletion of the day after the dust deposition. The nano- and microphytoplankton biomass increase was mainly due to *Haptophyceae* and *Chlorophyceae*, whereas the increase in picophytoplankton biomass mainly to *Haptophyceae* and *Cyanophyceae* (Table 1).

4 Discussion

4.1 Changes in the structure and composition of the phytoplankton community in response to dust additions

In pelagic ecosystems, the fluctuations in nutrient availability act at the level of numerous biological and ecological processes, and occur at different temporal and spatial scales, affecting intracellular biochemical properties and photosynthesis changes (Kolber et al., 1988; Davies and Grossman, 1998; Mock and Kroon, 2002), and relevantly controlling the phytoplankton community structure (Eppley and Peterson, 1979). The induced variations in such communities concern taxonomic, size and functional diversity, resulting in competition or coexistence of multiple species (Hutchinson, 1961; Tilman et al., 1982). Functional changes commonly regard changes in the phytoplankton cell size structure (and thus their elemental composition; Finkel et al., 2010), and the alternation of distinct functional groups diversified by peculiar biogeochemical properties (Iglesias-Rodriguez et al., 2002), also associated to the capacity of nitrogen-fixation (Le Quéré et al., 2005; Agawin et al., 2007) or diatom/cyanobacterial association (Carpenter et al., 1999), or even mixotrophy (Raven, 1997).

This cascade of biotic responses, spreading over large spatial and temporal scales, varies the abiotic properties and biodiversity of the ecosystem, with the ecophysiological characteristics of the successful species determining both the quality

BGD
9, 19199–19243, 2012

(elemental and biochemical composition) and quantity of primary production transferred up to the marine food web (Finkel et al., 2010 and references therein).

The aim of this work was to investigate how atmospheric new nutrient supplies would affect the growth capacity of the phytoplankton community of the surface layer in a LNLC area of the Mediterranean Sea, by coupling the study of functional features, as cell size or photobiological properties, with a size-dependent chemotaxonomic approach, through ChemTax pigment analysis (Rodriguez et al., 2006; Not et al., 2007). The dependency on micro-algal cell size of the ecosystem structure and functioning is well known and the contribution of the HPLC pigment determination on fractionated samples is relevant in providing size-related taxonomical information (e.g. Brunet and Lizon, 2003; Brunet et al., 2006, 2007). The approach used in this paper parallels flow cytometry with HPLC pigment measurements on fractionated samples to obtain deeper insights of cell size-related phytoplankton dynamics. Specifically, we investigated how the physiological state of a natural phytoplanktonic community, adapted to a high light climate (surface layer) and nutrient paucity (oligotrophic coastal system), would be modified by a sudden increase in nutrient availability.

The phytoplankton community responds to the two dust additions with distinct dynamics of structure and composition changes, linked to cell size constrains. Picophytoplankton respond to the first input of nutrients, while nano- and microphytoplankton response is mainly relevant soon after the second one. The rapid response of picophytoplankton fits their dominance and ability to out-compete bigger cells in oligotrophic conditions (as the case of the studied ecosystem) in relation to their greater capacity of physiological adaptation to extreme abiotic conditions (i.e. the nutrient-limitation and the high light pressure of the surface layer), relative to larger cell-sized phytoplankters (Raven, 1998; Raven et al., 2005). Because of a number of ecological and morphological peculiarities (e.g. the low surface area per unit volume and sinking rate), picophytoplankton are more effective in the acquisition and use of resources (i.e. photons and nutrients), determining their higher rates of cell division and physiological processes efficiency in low-resource habitats, when compared to bigger organisms.

BGD
9, 19199–19243, 2012

Our results show how this phytoplankton community is able to quickly and strongly respond to sudden new nutrient inputs, with *Cyanophyceae* and, to a lesser extent *Haptophyceae*, as the major players. This feature highlights the opportunistic behaviour of these groups under low-nutrient, low-chlorophyll and high light conditions, driven by allochthonous energy inputs. This first response does not induce any change in the community structure, being only a further increase of the already dominant picophytoplankton biomass, even if it leads to an enhancement of their contribution. In contrast, the larger cell-sized phytoplankton need three days to be able of a biomass increase, which is a quite long lag time that relates to the low biomass of nano- and microphytoplankton at the beginning of the experiment, possibly linked to the unhealthy physiological state of larger cells and competitive disadvantage relative to smaller ones. Nutrient concentration data show that nano- and microphytoplankton increase is strongly limited by the low concentration of nutrients present at the sea surface layer, after the picophytoplankton bloom in response to the first dust addition. A biomass increase of large cell size *Haptophyceae* and *Chlorophyceae*, even if slightly lower than the picophytoplankton biomass increase, relies upon the second pulse of nutrients, a response that causes a relevant enhancement of nano- and microphytoplankton biomass, contributing to ∼50 % of the total biomass. These results highlight that, in few days, the second dust addition caused relevant modifications in the ecological properties and trophic state of the first ten metres of the water column, with the chemical conditions of an oligotrophic system possibly switching into mesotrophic ones. Unfortunately, our experimental setup prevented us a meticulous investigation on the consequences of such changes in the phytoplankton community composition, by deepening the trophic web interactions.

In response to the second dust addition, the increase in greater cell size community biomass is not exclusive, and picophytoplankton are also able to grow, with prevalent contributions of *Haptophyceae*, *Cyanophyceae* and *Pelagophyceae*. The stronger increase in biomass of both phytoplanktonic size classes is related to the higher nutrient concentration in the water mass available after the second dust addition, than

BGD
9, 19199–19243, 2012

after the first one (please refer to Pulido-Villena et al., Ridame et al., Wuttig et al. and Guieu et al., 2012). This increase in total biomass needs all the available nutrients and exploits much higher concentrations of the two major macronutrients, i.e. nitrate ($-168.65\,\mu g\,NO_3^-\,L^{-1}\,d^{-1}$) and phosphate ($-7.7\,\mu g\,PO_4^{3-}\,L^{-1}\,d^{-1}$), relative to the biomass increase occurring after the first dust addition (Table 1), while the dissolved inorganic phosphate is also partially depleted by bacterial assimilation (Pulido-Villena et al., 2012). The estimated N/P ratio used for phytoplankton growth is ~22, i.e. relatively close to the Redfield ratio value.

During the first dust addition, a similar nitrogen ($[NO_3^-] + [NO_2^-]$)/phosphate ($[PO_4^{3-}]$) ratio characterizes both the picophytoplankton (84.3, increase of the second day) and the nano- and microphytoplankton nutrient assimilation (92, increase of the third day). We strongly believe that this result is due to nitrate limitation of the nano- and microplanktonic community, after the particularly long lag time for their growth response.

A striking result is that, among the > 3 µm size class, the response of *Chlorophyceae* importantly contributes to the biomass amount, despite being undetectable before the second dust addition took place or in control mesocosms. This finding could be explained by the high nutrient concentration-requirement of this class for growing. This is in agreement with the fact that the *Chlorophyceae*, at least for the picophytoplankton size class, are mainly found in DCM layers of oligotrophic ecosystems (Brunet et al., 2006, 2007). The hypothesis of their presence in the DCM was mainly related to their pigmentation, and notably the presence of Chl *b*, a pigment particularly suited to exploit the prevalently dim blue-light climate of such depths (Bidigare and Marra, 1990; Brunet et al., 2006). Thus, by comparing this study with the previous works (Brunet et al., 2006, 2007), we can assume that, in the case of the nano- or microphytoplanktonic cell size, the DCM low light climate is not the main trigger regulating the presence of *Chlorophyceae*, but rather their need of a nutrient concentration sufficiently high to grow. The presence of the pigment prasinoxanthin together with Chl *b* (data not shown) indicates that a portion of the Chl *b*-containing species is related to the prasinoxanthin-containing

BGD
9, 19199–19243, 2012

class *Prasinophyceae*, as already described within the water layer above 70 m depth in the Mediterranean Sea during summer (Brunet et al., 2006).

4.2 Effects of the dust additions on the physiological state of the phytoplankton community

Concomitant to changes in the composition and structure of the phytoplankton community, the physiological state of the community evolves, as shown by the increase of the pigment content per cell in picophytoplankton, a response that was also previously reported in LNLC region surface layers of the Atlantic Ocean (Davey et al., 2008; Moore et al., 2008).

By taking advantage of the absent detection of *Prochlorococcus*, the combination of HPLC-fractionated pigment and flow cytometry data allows us to estimate that the zeaxanthin (Zeax) content per *Synechococcus* cell ranged between 0.3 and 1.5 fg Zeax cell^{-1}, which is a lower range of values than the one reported by other studies (Kana et al., 1988; Morel et al., 1993; Moore et al., 1995). In these studies, the pigment content was obtained from laboratory-cultured species, i.e. under nutrient-replete conditions, and optimal temperature and light, which are all factors significantly affecting the pigment content of phytoplankton cells. Moreover, the data obtained in our work refer to samples collected in the upper water layer (from 0.1 to 10 m depth) and during summer, thus representative of a phytoplankton community undergoing quite extreme regimes of high light and oligotrophy. Indeed, our results show that increasing the concentration of nutrients in the water mass causes a rapid enhancement of the pigment content per cell, reflecting nutrient-dependent processes within the photosystems of *Synechococcus* cells, experiencing a healthy physiological state.

The chlorophyll (Chl) *a* content per picophytoplanktonic cell ranges from 1.5 to 3.4 fg Chl $a_{<3}$ cell^{-1}, increasing with the new nutrient inputs, as cellular physiological responses and/or species succession occur. Indeed, the contribution of *Synechococcus* is very high at the beginning of the experiment – explaining the low Chl *a* content per picophytoplankton cell – while the contribution of picoeukaryotic Chl *a* biomass

BGD
9, 19199–19243, 2012

of *Haptophyceae* and *Pelagophyceae* increases during the entire experiment. Brunet et al. (2006) have previously estimated values of Chl *a* content per picoeukaryotic cell (after excluding the *Synechococcus* contribution) of $\sim 10\,\mathrm{fg\,Chl}\,a\,\mathrm{cell}^{-1}$ in the surface water layer of the Mediterranean sea (with a depth between 10 and 25 m), while in cultures, values have been reported to vary between 50 and $150\,\mathrm{fg\,Chl}\,a\,\mathrm{cell}^{-1}$ (Dimier et al., 2007, 2009a, b; Giovagnetti et al., 2010). It should be highlighted that in situ studies (e.g. Brunet et al., 2006) dealing with photobiological properties of picoeukaryotes revealed a strong capacity of these small cells to modify their Chl *a* content in relation to the light climate, i.e. depth of the water mass, due to both species succession and physiological acclimation.

Concerning the nano- and microphytoplankton community, we report Chl *a* cellular content values ranging between 20 and $60\,\mathrm{fg\,Chl}\,a\,\mathrm{cell}^{-1}$. As found for the picophytoplankton community, the values of nano- and microphytoplankton Chl *a* cellular content are lower than the ones measured in laboratory cultures (Stolte et al., 2000), even under high light stress (LaRoche et al., 1991), possibly underlining the effect that nutrient-replete conditions might have on modifying the cellular pigment content in phytoplankton.

At the photophysiological level, a rapid photoprotective response (i.e. the development of non-photochemical fluorescence quenching; NPQ) is found soon after the first dust addition and remains quite high during few days, before decreasing due to nutrient concentration lowering. Several photophysiological mechanisms, either fast regulative (e.g. NPQ) or longer-term acclimative responses, adopted by algae to cope with high light or repair photodamage, involve the synthesis or modification of molecules (e.g. pigments or proteins) that requires energetic nutrient costs (e.g. Six et al., 2008; Raven, 2011).

The highest value of NPQ developed in response to the second dust addition might be due to the higher nutrient concentration reached at the surface and to the consequent higher contribution of nano- and micro-phytoplanktonic species, that might have a greater capacity to enhance NPQ than smaller ones (as the case of diatoms for

BGD
9, 19199–19243, 2012

instance; Brunet et al., 2011), after the second rather than the first dust addition. This finding might also be due to the overall decrease in *Cyanophyceae* contribution after the second dust addition, and to the fact that this group is not able to develop a strong NPQ relative to eukaryotic species (Brunet et al., 2011 and references therein), also in function of their high light adaptation, as they tend to occupy the surface water layer of oligotrophic areas, as also described in the Mediterranean Sea (Brunet et al., 2006, 2007).

Modifications of the physiological state of the phytoplankton community are furthermore underlined by comparing the maximal relative electron transport rate ($_{rel}ETR_{max}$) with the net primary production (^{13}C PP, see Ridame et al., 2012).

In control conditions, data of $_{rel}ETR_{max}$ and ^{13}C PP are significantly correlated, meaning that gross and net primary productions are related together, as expected for an optimal state of cell physiological adaptation to the abiotic environmental conditions. This result reveals the good fitness between ecophysiological requirements of the phytoplankton community – mainly constituted by picophytoplankton – and the surrounding ecosystem.

When nutrients are added to the system, the net primary production increases, and two distinct responses can be found, depending on phytoplankton cell size constrains. During the first dust addition, when the community is largely dominated by picophytoplankton, and among them *Cyanophyceae*, the net primary production increase is not related to an enhanced ETR within the photosystem (PS) II, but probably to a more efficient use of the products synthesized during the photosynthetic reactions (e.g. by the decreasing the photorespiration rate). In this case, the increase in primary production of picophytoplankton, i.e. the greater uptake of nutrients mainly by *Haptophyceae* and *Cyanophyceae*, is not due to an increase in the flux of electrons within the PSII, but probably to a more efficient regulative strategy to produce biomass. We can thus hypothesize that the new nutrient inputs would act primarily on carbon reduction reactions (at the level of the Calvin Cycle), rather than on early photon harvesting and excitation energy transfer within the PSII.

BGD
9, 19199–19243, 2012

In contrast, the stronger increase in nano- and microphytoplankton biomass after the second than the first dust addition might be the reason why $_{rel}ETR_{max}$ and ^{13}C PP are significantly correlated. This result might suggest that, in a community in which the abundance of large-sized cells becomes relevant, the observed increase in both net and gross primary production is driven by a PSII ETR enhancement, indicating the direct effect of nutrient limitation on the light-harvesting capacity and/or the excitation energy transfer within PSII.

We may therefore infer that the regulation of photobiological processes is distinctively affected by nutrient availability in both phytoplanktonic size classes, in agreement with previous studies (Mei et al., 2009; Chen and Liu, 2010) that recall the metabolic theory of ecology (Brown et al., 2004). Insofar, regulative physiological and biochemical mechanisms, activated during nutrient limitation or repletion regimes, would operate at two different levels of the photosynthetic process, in relation to phytoplankton cell-size dependent energy-requirements of biomass synthesis.

Our results demonstrate that dust additions are a relevant source of abiotic and biotic energy in the upper mixed layer, causing significant changes in the phytoplankton community over time. Picophytoplankton are the first group responding to such dust additions, in terms of both ecophysiological state of cells and community composition. On the contrary, bigger-sized cells need a further nutrient supply for being able to adjust their physiology and compete for resource acquisition and biomass increase. Because such changes might significantly affect the functioning and productivity of LNLC ecosystems, we can hypothesize that multiple dust additions, quantitatively and qualitatively comparable to the ones performed during this experiment, and occurring on a large area of the Mediterranean Sea (Bergametti et al., 1989; Guieu et al., 2010a), might cause an increase in the regional budget of the exported carbon, eventually influencing the functioning of the Mediterranean pelagic ecosystem.

Acknowledgements. This work was funded by the ANR-DUNE under the contract "ANR-07-BLAN-30 0126-01". V. Giovagnetti's PhD was financially supported by the Stazione Zoologica A. Dohrn. J.M. Dominici and collaborators of the "Réserve naturelle de Scandola, Parc naturel

BGD
9, 19199–19243, 2012

régional de Corse" are gratefully acknowledged for their help and cooperation in performing the experiments and implementing the field work conducted in the bay of Elbo. The authors would like to deeply thank all the participants of the DUNE-2 project for their involvement in developing the experimental design and performing the experiments.

References

Agawin, N. S. R., Rabouille, S., Veldhuis, M. J. W., Servatius, L., Hol, S., Overzee, H. M. J., and Huisman, J.: Competition and facilitation between unicellular nitrogen-fixing cyanobacteria and non-nitrogen-fixing phytoplankton species, Limnol. Oceanogr., 52, 2233–2248, 2007.

Agogué, H., Casamayor, E. O., Joux, F., Obernosterer, I., Dupuy, C., Lantoine, F., Catala, P., Weinbauer, M. G., Rheinthaler, T., Herndl, G. J., and Lebaron, P.: Comparison of samplers for the biological characterization of the sea surface microlayer, Limnol. Oceanogr.-Meth., 2, 213–225, 2004.

Bartoli, G., Migon, C., and Losno, R.: Atmospheric input of dissolved inorganic phosphorus and silicon to the coastal northwestern Mediterranean Sea: fluxes, variability and possible impact on phytoplankton dynamics, Deep-Sea Res. Pt. I, 52, 2005–2016, 2005.

Bergametti, G., Dutot, A. L., Buat-Menard, P., Losno, R., and Remoudaki, E.: Seasonal variability of the elemental composition of atmospheric aerosol particles over the northwestern Mediterranean, Tellus B, 41, 353–361, 1989.

Bergametti, G., E. Remoudaki, R. Losno, E. Steiner, and Chatenet, B.: Source, transport and deposition of atmospheric phosphorus over the northwestern Mediterranean, J. Atmos. Chem., 14, 501–513, doi:10.1007/BF00115254, 1992.

Bidigare, R. R. and Marra, J.: Evidence for phytoplankton succession and chromatic in the Sargasso sea during spring 1985, Mar. Ecol.-Prog. Ser., 60, 113–122, 1990.

Blain, S., Guieu, C., Claustre, H., Leblanc, K., Moutin, T., Quéguiner, B., Ras, J., and Sarthou, G.: Availability of iron and major nutrients for phytoplankton in the northeast Atlantic Ocean, Limnol. Oceanogr., 49, 2095–2104, 2004.

Blain, S., Bonnet, S., and Guieu, C.: Dissolved iron distribution in the tropical and sub tropical South Eastern Pacific, Biogeosciences, 5, 269–280, doi:10.5194/bg-5-269-2008, 2008.

BGD
9, 19199–19243, 2012

Bonnet, S., Guieu, C., Chiaverini, J., Ras, J., and Stock, A.: Effect of atmospheric nutrients on the autotrophic communities in a low nutrient, low chlorophyll system, Limnol. Oceanogr., 50, 1810–1819, 2005.

Boyd, P. W., Jickells, T., Law, C. S., Blain, S., Boyle, E. A., Buesseler, K. O., Coale, K. H., Cullen, J. J., de Baar, H. J. W., Follows, M., Harvey, M., Lancelot, C., Levasseur, M., Owens, N. P. J., Pollard, R., Rivkin, R. B., Sarmiento, J., Schoemann, V., Smetacek, V., Takeda, S., Tsuda, A., Turner, S., and Watson, A. J.: Mesoscale iron enrichment experiments 1993–2005: Synthesis and future directions, Science, 315, 612–617, 2007.

Brown, J. H., Gillooly, J. F., Allen, A. P., Savage, V. M., and West, G. B.: Toward a metabolic theory of ecology, Ecology, 85, 1771–1789, 2004.

Brunet, C. and Lizon, F.: Tidal and diel periodicities of size fractionated phytoplankton pigment signatures at an offshore station in the South-Eastern English Channel, Estuar. Coast. S., 56, 835–845, 2003.

Brunet, C., Casotti, R., Vantrepotte, V., Corato, F., and Conversano, F.: Picophytoplankton diversity and photophysiology in the Strait of Sicily (Mediterranean Sea) in summer. I. Mesoscale variations, Aquat. Microb. Ecol., 44, 127–141, 2006.

Brunet, C., Casotti, R., Vantrepotte, V., and Conversano, F.: Vertical variability and diel dynamics of picophytoplankton in the Strait of Sicily (Mediterranean Sea) in summer, Mar. Ecol.-Prog. Ser., 346, 15–26, 2007.

Brunet, C., Casotti, R., and Vantrepotte, V.: Phytoplankton diel and vertical variability in photobiological responses at a coastal station in the Mediterranean Sea, J. Plankton Res., 30, 645–654, 2008.

Brunet, C., Johnsen, G., Lavaud, J., and Roy, S.: Selected pigment applications in oceanography Pigments and photoacclimation processes, in: Phytoplankton Pigments in Oceanography: Guidelines to Modern Methods, Series: Oceanographic Methodologies, Vol. 2, edited by: Roy, S., Johnsen, G., Llewellyn, C., and Skarstad, E., SCOR-UNESCO, Publishing, Cambridge University Press, 2011.

Carpenter, E. J., Montoya, J. P., Burns, J., Mulholland, M. R., Subramaniam, A., and Capone, D. G.: Extensive bloom of a N_2-fixing diatom/cyanobacterial association in the tropical Atlantic Ocean, Mar. Ecol.-Prog. Ser., 185, 273–83, 1999.

Casotti, R., Landolfi, A., Brunet, C., D'Ortenzio, F., Mangoni, O., Boldrin, A., Ribera d'Alcalà, M. and Denis, M.: Composition and dynamics of the phytoplankton of the Ionan Sea (Eastern Mediterranean), J. Geophys. Res., 108, 1–19, 2003.

BGD
9, 19199–19243, 2012

Chen, B. Z. and Liu, H. B.: Relationships between phytoplankton growth and cell size in surface oceans: interactive effects of temperature, nutrients, and grazing, Limnol. Oceanogr., 55, 965–972, 2010.
Chisholm, S. W., Olson, R. J., Zettler, E. R., Goericke, R., Waterbury, J. B., and Welschmeyer, N. A.: A novel free-living prochlorophyte abundant in the oceanic euphotic zone, Nature, 334, 340–343, 1988.
Chisholm, S. W., Frankel, S. L., Goericke, R., Olson, R. J., Palenik, B., Waterbury, J. B., West-Johnsrud, L., and Zettler, E. R.: *Prochlorococcus marinus* nav. gen. nov. sp., an oxytrophic marine prokaryote containing divinyl chlorophyll *a* and *b*, Arch. Mikrobiol., 157, 297–300, 1992.
Cullen, J. J.: The deep chlorophyll maximum: comparing vertical profiles of chlorophyll *a*, Can. J. Fish. Aquat. Sci., 39, 791–803, 1982.
Davey, M., Tarran, G. A., Mills, M. M., Ridame, C., Geider, R. J., and LaRoche, J.: Nutrient limitation of picophytoplankton photosynthesis and growth in the tropical North Atlantic, Limnol. Oceanogr., 53, 1722–1733, 2008.
Davies, J. P. and Grossman, A. R.: Responses to deficiencies in macronutrients, in: The Molecular Biology of Chloroplast and Mitochondria in *Chlamydomonas*, edited by: Goldschmidt-Clermont, M. and Merchant, S., Kluwer Academic Publishers, Amsterdam, The Netherlands, 613–633, 1998.
Díez, B., Pedrós-Alió, C., and Massana, R.: Study of genetic diversity of eukaryotic picoplankton in different oceanic regions by small-subunit rRNA gene cloning and sequencing, Appl. Environ. Microbiol., 67, 2932–2941, 2001.
Dimier, C., Corato, F., Saviello, G., and Brunet, C.: Photophysiological properties of the marine picoeukaryote Picochlorum CC237 (*Trebouxiophyceae*, Chlorophyta), J. Phycol., 43, 275–283, 2007.
Dimier, C., Brunet, C., Geider, J. R., and Raven, J. A.: Growth and photoregulation dynamics of the picoeukaryote *Pelagomonas calceolata* in fluctuating light, Limnol. Oceanogr., 54, 823–836, 2009a
Dimier, C., Saviello, G., Tramontano, F., and Brunet, C.: Comparative ecophysiology of the xanthophyll cycle in six marine phytoplanktonic species, Protist, 160, 397–411, 2009b
Duce, R. A., Liss, P. S., Merrill, J. T., Atlas, E. L., Buat-Menard, P., Hicks, B. B., Miller, J. M., Prospero, J. M., Arimoto, R., Church, T. M., Ellis, W., Galloway, J. N., Hansen, L., Jickells, T. D., Knap, A. H., Reinhardt, K. H., Schneider, B., Soudine, A., Tokos, J. J., Tsunogai, S., Wol-

BGD
9, 19199–19243, 2012

last, R., and Zhou, M.: The atmospheric input of trace species to the world ocean, Global Biogeochem. Cy., 5, 193–259, 1991.
Dugdale, R. C. and Goering, J. J.: Uptake of new and regenerated forms of nitrogen in primary productivity, Limnol. Oceanogr., 12, 196–206, 1967.
Eilers, P. H. C. and Peeters, J. C. H.: A model for the relationship between light intensity and the rate of photosynthesis in phytoplankton, Ecol. Model., 42, 199–215, 1988.
Eppley, R. W. and Peterson, B. J.: Particulate organic matter flux and planktonic new production in the deep ocean, Nature, 282, 677–680, 1979.
Finkel, Z. V., Beardall, J., Flynn, K. J., Quigg, A., Rees, T. A., and Raven, J. A.: Phytoplankton in a changing world: cell size and elemental stoichiometry, J. Plankton Res., 32, 119–137, 2010.
Giovagnetti, V., Cataldo, M. L., Conversano, F., and Brunet, C.: Functional relation between growth, photosynthetic rate and regulation in the coastal picoeukaryote *Phaeomonas* sp. RCC 503 (*Pinguiophyceae*, Stramenopiles), J. Plankton Res., 32, 1501–1511, 2010.
Giovagnetti, V., Cataldo, M. L., Conversano, F., and Brunet, C.: Growth and photophysiological responses of two picoplanktonic *Minutocellus* species, strains RCC967 and RCC703 (*Bacillariophyceae*), Eur. J. Phycol., 47, 408–420, 2012.
Gould, R. W.: The deep chlorophyll maximum in the world ocean: a review, Biologist, 66, 4–13, 1987.
Guerzoni, S., Chester, R., Dulac, F., Herut, B., Loye-Pilot, M. D., Measures, C., Migon, C., Molinaroli, E., Moulin, C., Rossini, P., Saydam, C., Soudine, A., and Ziveri, P.: The role of atmospheric deposition in the biogeochemistry of the Mediterranean Sea, Prog. Oceanogr., 44, 147–190, 1999.
Guieu, C., Loÿe-Pilot, M.-D., Ridame, C., and Thomas, C.: Chemical characterization of the Saharan dust end-member: some biogeochemical implications for the western Mediterranean Sea, J. Geophys. Res., 107, 4258, doi:10.1029/2001JD000582, 2002.
Guieu, C., Loÿe-Pilot, M.-D., Benyaya, L., and Dufour, A.: Spatial variability of atmospheric fluxes of metals (Al, Fe, Cd, Zn and Pb) and phosphorus over the whole Mediterranean from a one year monitoring experiment: biogeochemical implications, Mar. Chem., 120, 164–178, 2010a.
Guieu, C., Dulac, F., Desboeufs, K., Wagener, T., Pulido-Villena, E., Grisoni, J.-M., Louis, F., Ridame, C., Blain, S., Brunet, C., Bon Nguyen, E., Tran, S., Labiadh, M., and Dominici, J.-M.: Large clean mesocosms and simulated dust deposition: a new methodology to investi-

BGD
9, 19199–19243, 2012

gate responses of marine oligotrophic ecosystems to atmospheric inputs, Biogeosciences, 7, 2765–2784, doi:10.5194/bg-7-2765-2010, 2010.
Guieu, C., Dulac, F., Ridame, C., and Pondaven, P.: An introduction to the dune project, Biogeosciences, in preparation, 2012.
Hofstraat, J. W., Peeters, J. C. H., Snel, J. F. H., and Geel, C.: Simple determination of photosynthetic efficiency and photoinhibition of *Dunaliella tertiolecta* by saturating pulse fluorescence measurements, Mar. Ecol.-Prog. Ser., 103, 187–196, 1994.
Hutchinson, G. E.: The paradox of the plankton, Am. Nat., 95, 137–145, 1961.
Iglesias-Rodriguez, D. M., Brown, C. W., Doney, S. C., Kleypas, J. A., Kolber, D., Kolber, Z., Hayes, P. K., and Falkowski, P. G.: Representing key phytoplankton functional groups in ocean carbon cycle models: Coccolithophorids, Global Biogeochem. Cy., 16, 1–20, 2002.
Kana, T. M., Glibert, P. M., Goericke, R., and Welschmeyer, N. A.: Zeaxanthin and β carotene in *Synechococcus* WH 7803 respond differently to irradiance, Limnol. Oceanogr., 33, 1623–1627, 1988.
Kirk, J. T. O.: Light and Photosynthesis in Aquatic Ecosystems, 2nd. edn., Cambridge University Press, Cambridge, 509 pp., 1994.
LaRoche, J., Mortain-Bertrand, A., and Falkowski, P. G.: Light intensity-induced changes in cab mRNA and light harvesting complex 11 apoprotein levels in the unicellular chlorophyte *Dunaliella tertiolecta*, Plant Physiol., 97, 147–153, 1991.
Law, C. S., Woodward, E. M. S., Ellwood, M. J., Marriner, A., Bury, S. J., and Safi, K. A.: Response of surface nutrient inventories and nitrogen fixation to a tropical cyclone in the southwest Pacific, Limnol. Oceanogr., 56, 1372–1385, 2011.
Le Gall, F., Rigaut-Jalabert, F., Marie, D., Garczarek, L., Viprey, M., Gobet, A., and Vaulot, D.: Picoplankton diversity in the South-East Pacific Ocean from cultures, Biogeosciences, 5, 203–214, doi:10.5194/bg-5-203-2008, 2008.
Le Quéré, C., Harrison, S. P., Prentice, I. C., Buitenhuis, E. T., Aumont, O., Bopp, L., Claustre, H., Da Cunha, L. C., Geider, R. J., Giraud, X., Klaas, C., Kohfeld, K. E., Legendre, L., Manizza, M., Platt, T., Rivkin, R. B., Sathyendranath, S., Uitz, J., Watson, A. J., and Wolf-Gladrow, D.: Ecosystem dynamics based on plankton functional types for global ocean biogeochemistry models, Glob. Change Biol., 11, 2016–2040, 2005.
Magazzù, G. and Decembri, F.: Primary production, biomass and abundance of phototrophic picoplankton in the Mediterranean Sea: a review, Aquat. Microb. Ecol., 9, 97–104, 1995.

BGD
9, 19199–19243, 2012

Marañón, E.: Phytoplankton growth rates in the Atlantic subtropical gyres, Limnol. Oceanogr., 50, 299–310, 2005.
Marañón, E., Fernández, A., Mouriño-Carballido, B., Martínez-García, S., Teira, E., Cermeño, P., Chouciño, P., Huete-Ortega, M., Fernández, E., Calvo-Díaz, A., Morán, X. A. G., Bode, A., Moreno-Ostos, E., Varela, M. M., Patey, M. D., and Achterberg, E. P.: Degree of oligotrophy controls the response of microbial plankton to Saharan dust, Limnol. Oceanogr., 55, 2339–2352, 2010.
Marie, D., Simon, N., Guillou, L., Partensky, F., and Vaulot, D.: Flow cytometry analysis of marine picoplankton, in: Living Color: Protocols in Flow Cytometry and Cell Sorting, edited by: De Maggio, Springer Verlag, Berlin, 421–454, 2000.
Marinov, I., Doney, S. C., and Lima, I. D.: Response of ocean phytoplankton community structure to climate change over the 21st century: partitioning the effects of nutrients, temperature and light, Biogeosciences, 7, 3941–3959, doi:10.5194/bg-7-3941-2010, 2010.
Mei, Z.-P., Finkel, Z. V., and Irwin, A.: Light and nutrient availability affect the size-scaling of growth in phytoplankton, J. Theor. Biol., 259, 582–588, 2009.
Mills, M. M., Ridame, C., Davey, M., La Roche, J., and Geider, R. J.: Iron and phosphorus co-limit nitrogen fixation in the eastern tropical North Atlantic, Nature, 429, 292–294, 2004.
Mock, T. and Kroon, B. M. A.: Photosynthetic energy conversion under extreme conditions-II: the significance of lipids under light limited growth in Antarctic sea ice diatoms, Phytochemistry, 61, 53–60, 2002.
Moon-van der Staay, S. Y., De Wachter, R., and Vaulot, D.: Oceanic 18S rDNA sequences from picoplankton reveal unsuspected eukaryotic diversity, Nature, 409, 607–610, 2001.
Moore, L. R., Goericke, R., and Chisholm, S. W.: Comparative physiology of *Synechococcus* and *Prochlorococcus*: influence of light and temperature on growth, pigments, fluorescence and absorptive properties, Mar. Ecol.-Prog. Ser., 116, 259–275, 1995.
Moore, C. M., Mills, M. M., Langlois, R., Milne, A., Achterger, E. P., LaRoche, J., and Geider, R. J.: Relative influence of nitrogen and phosphorus availability on phytoplankton physiology and productivity in the oligotrophic sub-tropical North Atlantic Ocean, Limnol. Oceanogr., 53, 291–305, 2008.
Morel, A., Ahn, Y. H., Partensky, F., Vaulot, D., and Claustre, H.: *Prochlorococcus* and *Synechococcus*: a comparative study of their optical properties in relation to their size and pigmentation, J. Mar. Res., 51, 617–649, 1993.

BGD
9, 19199–19243, 2012

Not, F., Simon, N., Biegala, I. C., and Vaulot, D.: Application of fluorescent in situ hybridization coupled with tyramide signal amplification (FISH-TSA) to assess eukaryotic picoplankton composition, Aquat. Microb. Ecol., 28, 157–166, 2002.
Not, F., Massana, R., Latasa, M., Marie, D., Colson, C., Eikrem, W., Pedrós-Alió, C., Vaulot, D., and Simon, N.: A late summer community composition and abundance of photosynthetic picoeukaryotes in Norwegian and Barents Sea, Limnol. Oceanogr., 50, 1677–1686, 2005.
Not, F., Zapata, M., Pazos, Y., Campana, E., Doval, M., and Rodriguez, F.: Size-fractionated phytoplankton diversity in the NW Iberian cost: a combination of microscopic, pigment and molecular analyses, Aquat. Microb. Ecol., 40, 255–265, 2007.
Paerl, H. W., Willey, J. D., Go, M., Peierls, B. L., Pinckney, J. L., and Fogel, M. L.: Rainfall stimulation of primary production in western Atlantic Ocean waters: roles of different nitrogen sources and co-limiting nutrients, Mar. Ecol.-Prog. Ser., 176, 205–214, 1999.
Partensky, F., Blanchot, J., and Vaulot, D.: Differential distribution and ecology of *Prochlorococcus* and *Synechococcus* in oceanic waters: a review, Bull. Inst. Oceanogr. Monaco Numero Spec., 19, 431–449, 1999
Pérez, V., Fernández, E., Marañón, E., Morán, X. A. G., and Zubkov, M. V.: Vertical distribution of phytoplankton biomass, production and growth in the Atlantic subtropical gyres, Deep-Sea Res. Pt. I, 53, 1616–1634, 2006.
Pulido-Villena, E., Wagener, T., and Guieu, C.: Bacterial response to dust pulses in the western Mediterranean: implications for carbon cycling in the oligotrophic ocean, Global Biogeochem. Cy., 22, GB1020, doi:10.1029/2007GB003091, 2008.
Pulido-Villena, E., Baudoux, A. C., Obernosterer, I., and Guieu, C.: Enhanced bacterial mineralization of organic matter after a dust event: results from a mesocosm study, Biogeosciences, in preparation, 2012.
Raven, J. A.: Phagotrophy in autotrophs, Limnol. Oceanogr., 42, 198–205, 1997.
Raven, J. A.: The twelfth Tansley lecture. Small is beautiful: the picophytoplankton, Funct. Ecol., 12, 503–513, 1998.
Raven, J. A.: The cost of photoinhibition, Physiol. Plantarum, 142, 87–104, 2011
Raven, J. A., Finkel, Z. V., and Irwin, A. J.: Picophytoplankton: bottom-up and top-down controls on ecology and evolution, Vie Milieu, 55, 209–215, 2005.
Ridame, C. and Guieu, C.: Saharan input of phosphate to the oligotrophic water of the open western Mediterranean Sea, Limnol. Oceanogr., 47, 856–869, 2002.

BGD
9, 19199–19243, 2012

Ridame, C., Pulido-Villena, E., and Guieu, C.: Phytoplankton responses to contrasted Saharan dust events: results from dust fertilizations in large mesocosms, Biogeosciences, in preparation, 2012.
Rodriguez, F., Garrido, J. L., Crespo, B. G., Arbones, B., and Figueiras, F. G.: Size-fractionated phytoplankton pigment groups in the NW Iberian upwelling system: impact of the Iberian Poleward current, Mar. Ecol.-Prog. Ser., 323, 59–73, 2006
Schreiber, U., Bilger, W., and Neubauer, C.: Chlorophyll fluorescence as a non-intrusive indicator for rapid assessment of in vivo photosynthesis, Ecol. Studies, 100, 49–70, 1994.
Six, C., Finkel, Z. V., Rodriguez, F., Marie, D., Partensky, F., and Campbell, D. A.: Contrasting photoacclimation costs in ecotypes of the marine eukaryote picoplankter *Ostreococcus*, Limnol. Oceanogr., 53, 255–265, 2008.
Six, C., Sherrard, R., Lionard, M., Roy, S., and Campbell, D. A.: Photosystem II and pigment dynamics among ecotypes of the green alga *Ostreococcus*, Plant Physiol., 151, 379–390, 2009.
Stolte, W., Kraay, G. W., Noordeloos, A. A. M., and Riegman, R.: Genetic and physiological variation in pigment composition of *Emiliania huxleyi* (*Prymnesiophyceae*) and the potential use of its pigment ratios as a quantitative physiological marker, J. Phycol., 36, 529–539, 2000.
Tilman, D., Kilham, S. S., and Kilham, P.: Phytoplankton community ecology: the role of limiting nutrients, Annu. Rev. Ecol. Syst., 13, 349–72, 1982.
Vaulot, D., Eikrem, W., Viprey, M., and Moreau, H.: The diversity of small eukaryotic phytoplankton ($\leq 3\,\mu m$) in marine ecosystems, FEMS Microbiol. Rev., 32 795–820, 2008.
Veldhuis, M. J. W. and Kraay, G. W.: Vertical distribution and pigment composition of picoplanktonic prochlorophyte in the subtropical North Atlantic: a combined study of HPLC analysis of pigments and flow cytometry, Mar. Ecol.-Prog. Ser., 68, 121–127, 1990.
Wagener, T., Guieu, C., and Leblond, N.: Effects of dust deposition on iron cycle in the surface Mediterranean Sea: results from a mesocosm seeding experiment, Biogeosciences, 7, 3769–3781, doi:10.5194/bg-7-3769-2010, 2010.
Waterbury, J. B., Watson, S. W., Guillard, R. R., and Brand, L. E.: Widespread occurrence of a unicellular marine plankton cyanobacteria, Nature, 277, 293–294, 1979.
Wedepohl, K.: The composition of the continental crust, Geochim. Cosmochim. Acta, 59, 1217–1232, 1995.

BGD
9, 19199–19243, 2012

Worden, A. Z. and Not, F.: Ecology and diversity of picoeukaryotes, in: Microbial Ecology of the Oceans, 2nd. edn, edited by: Kirchman, D. L., Wiley, Hoboken, NJ, 159–205, 2008.
Wuttig, K., Wagener, T., Bressac, M., Dammshäuser, A., Streu, P., Guieu, C., and Croot, P. L.: Impacts of dust deposition on dissolved trace metal concentrations (Mn, Al and Fe) during a mesocosm experiment, Biogeosciences Discuss., 9, 13857–13897, doi:10.5194/bgd-9-13857-2012, 2012.

BGD
9, 19199–19243, 2012

Table 1. Daily variation of total and fractionated chlorophyll (Chl) *a* concentration ($\mu g\,Chl\,a\,L^{-1}\,d^{-1}$), dominant phytoplanktonic groups ($\mu g\,Chl\,a\,L^{-1}\,d^{-1}$), and nutrients concentration ($\mu g\,nutrient\,L^{-1}\,d^{-1}$), two (47 h) and three days (71 h) after the first dust addition, and the day (191 h) after the second dust addition. Δ [Chl a_{Tot}], variation of total chlorophyll *a* concentration; Δ Chl $a_{<3}$, variation of picophytoplankton chlorophyll *a* concentration; Δ [Chl $a_{>3}$], variation of nano-/microphytoplankton chlorophyll *a* concentration. Daily variations have been calculated on mean values of the data measured at 0.1 and 5 m depths. Chloro, *Chlorophyceae*; Cyano, *Cyanophyceae*; Dino, *Dinophyceae*; Hapto, *Haptophyceae*; Pelago, *Pelagophyceae*. NO_3^-, nitrate; NO_2^-, nitrite; PO_4^{3-}, phosphate; SiO_2, silicon dioxide; DFe, dissolved iron.

Time	Δ[Chl a_{Tot}]	Δ[Chl $a_{<3}$]	Δ[Chl $a_{>3}$]	NO_3^-	PO_4^{3-}	NO_2^-	SiO_2	DFe
First seeding								
47	0.0077	0.0077 **Hapto$_{<3}$** (23 %) **Cyano$_{<3}$** (77 %)	0.000	−38.1	−0.46	−0.67	−12.3	−0.035
71	−0.0058	−0.0085	0.0027 **Dino$_{>3}$** (55 %) **Hapto$_{>3}$** (45 %)	−15.5	−0.17	−0.14	−2.31	−0.042
Second seeding								
191	0.027	0.0157 **Hapto$_{<3}$** (51 %) **Cyano$_{<3}$** (36 %) **Pelago$_{<3}$** (13 %)	0.0114 **Hapto$_{>3}$** (47 %) **Chloro$_{>3}$** (42 %) **Dino$_{>3}$** (11 %)	−168.6	−7.7	−0.85	−1.50	−0.007

BGD
9, 19199–19243, 2012

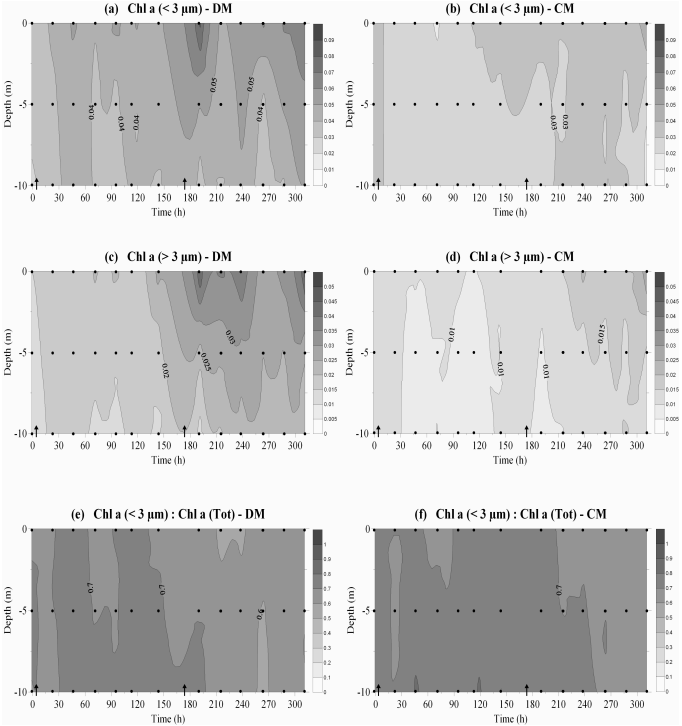

Fig. 1. Evolution of picophytoplankton mean chlorophyll (Chl) $a_{<3}$ concentration (µg Chl $a_{<3}$ L^{-1}) in dust-amended mesocosms (DM; **a**) and control mesocosms (CM; **b**), nano- and microphytoplankton mean Chl $a_{>3}$ concentration (µg Chl $a_{>3}$ L^{-1}) in DM **(c)** and CM **(d)**, and picophytoplankton biomass contribution to total phytoplankton biomass (Chl $a_{<3}$: Chl a_{Tot}) in DM **(e)** and CM **(f)**, over time (h). The arrows indicate the time at which each dust addition was performed.

BGD
9, 19199–19243, 2012

Assessing the role of dust deposition on phytoplankton ecophysiology

V. Giovagnetti et al.

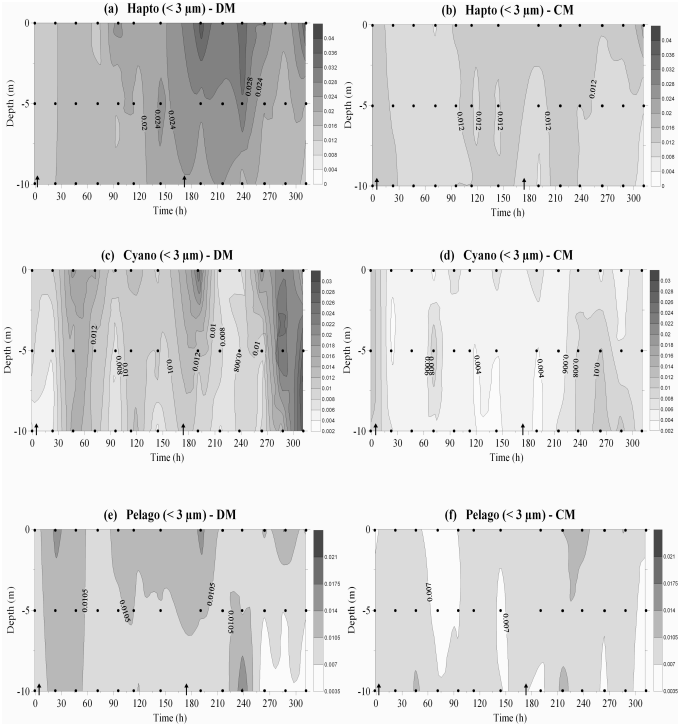

Fig. 2. Evolution of picophytoplanktonic *Haptophyceae* mean chlorophyll (Chl) $a_{<3}$ concentration ($\mu g\,Chl\,a_{<3}\,L^{-1}$) in dust-amended mesocosms (DM; **a**) and control mesocosms (CM; **b**), *Cyanophyceae* mean Chl $a_{<3}$ concentration ($\mu g\,Chl\,a_{<3}\,L^{-1}$) in DM **(c)** and CM **(d)**, and *Pelagophyceae* mean Chl $a_{<3}$ concentration ($\mu g\,Chl\,a_{<3}\,L^{-1}$) in DM **(e)** and CM **(f)**, over time (h). The biomass of each picophytoplanktonic group was obtained through ChemTax analysis. Cyano, *Cyanophyceae*; Hapto, *Haptophyceae*; Pelago, *Pelagophyceae*. The arrows indicate the time at which each dust addition was performed.

BGD
9, 19199–19243, 2012

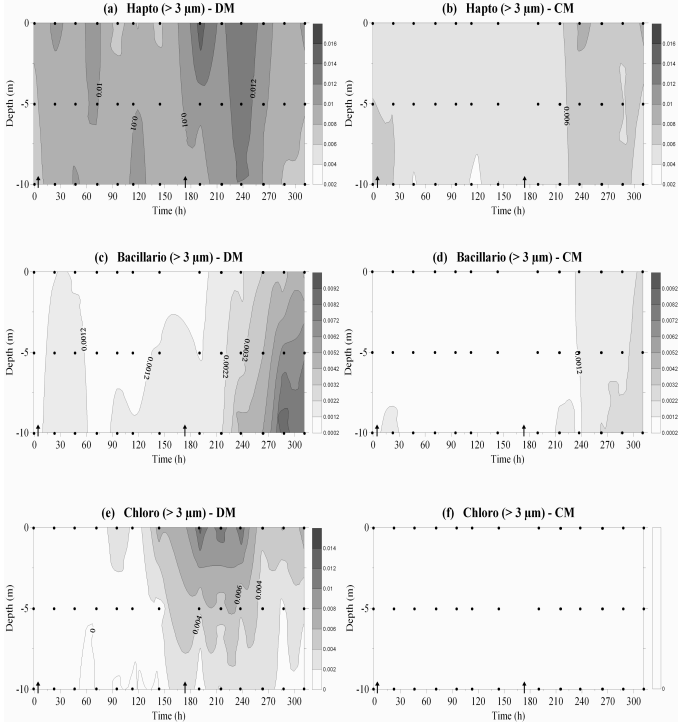

Fig. 3. Evolution of nano- and microphytoplanktonic *Haptophyceae* mean chlorophyll (Chl) $a_{>3}$ concentration ($\mu g\,Chl\,a_{>3}\,L^{-1}$) in dust-amended mesocosms (DM; **a**) and control mesocosms (CM; **b**), *Bacillariophyceae* mean Chl $a_{>3}$ concentration ($\mu g\,Chl\,a_{>3}\,L^{-1}$) in DM **(c)** and CM **(d)**, and *Chlorophyceae* mean Chl $a_{>3}$ concentration ($\mu g\,Chl\,a_{>3}\,L^{-1}$) in DM **(e)** and CM **(f)**, over time (h). The biomass of each nano- and microphytoplanktonic group was obtained through Chem-Tax analysis. Bacillario, *Bacillariophyceae*; Chloro, *Chlorophyceae*; Hapto, *Haptophyceae*. The arrows indicate the time at which each dust addition was performed.

BGD
9, 19199–19243, 2012

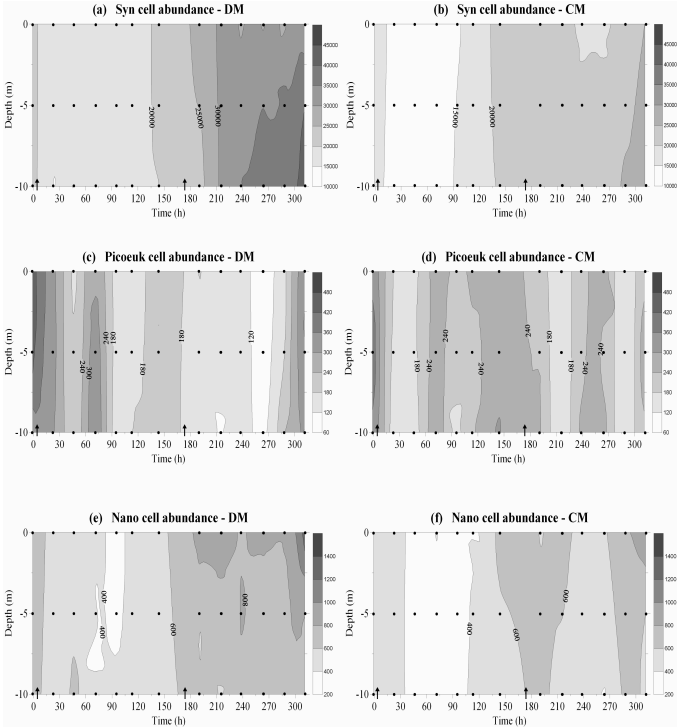

Fig. 4. Evolution of *Synechococcus* mean cell abundance (cells mL^{-1}) in dust-amended mesocosms (DM; **a**) and control mesocosms (CM; **b**), picoeukaryotes mean cell abundance (cells mL^{-1}) in DM **(c)** and CM **(d)**, and nanophytoplankton mean cell abundance (cells mL^{-1}) in DM **(e)** and CM **(f)**, over time (h). Syn, *Synechococcus*; Picoeuk, picoeukaryotes; Nano, nanophytoplankton. The arrows indicate the time at which each dust addition was performed.

BGD
9, 19199–19243, 2012

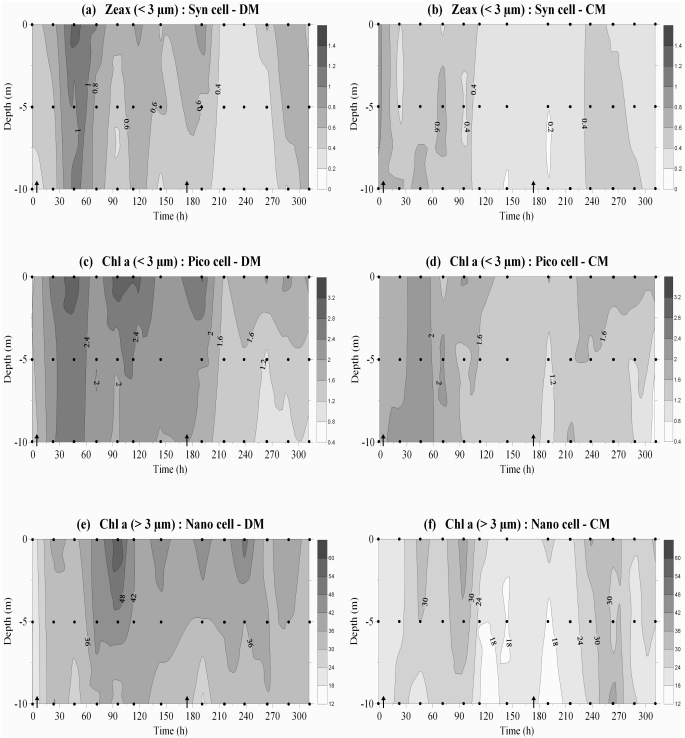

Fig. 5. Evolution of picophytoplankton mean zeaxanthin ($Zeax_{<3}$) concentration per *Synechococcus* cell abundance (fg $Zeax_{<3}$ cell^{-1}) in dust-amended mesocosms (DM; **a**) and control mesocosms (CM; **b**), picophytoplankton mean chlorophyll (Chl) $a_{<3}$ concentration per the sum of *Synechococcus* and picoeukaryotes cell abundance (fg Chl $a_{<3}$ cell^{-1}) in DM **(c)** and CM **(d)**, and nanophytoplankton mean Chl $a_{>3}$ concentration per cell abundance (fg Chl $a_{>3}$ cell^{-1}) in DM **(e)** and CM **(f)**, over time (h). Syn, *Synechococcus*; Pico, picophytoplankton; Nano, nanophytoplankton. The arrows indicate the time at which each dust addition was performed.

BGD
9, 19199–19243, 2012

Assessing the role of dust deposition on phytoplankton ecophysiology

V. Giovagnetti et al.

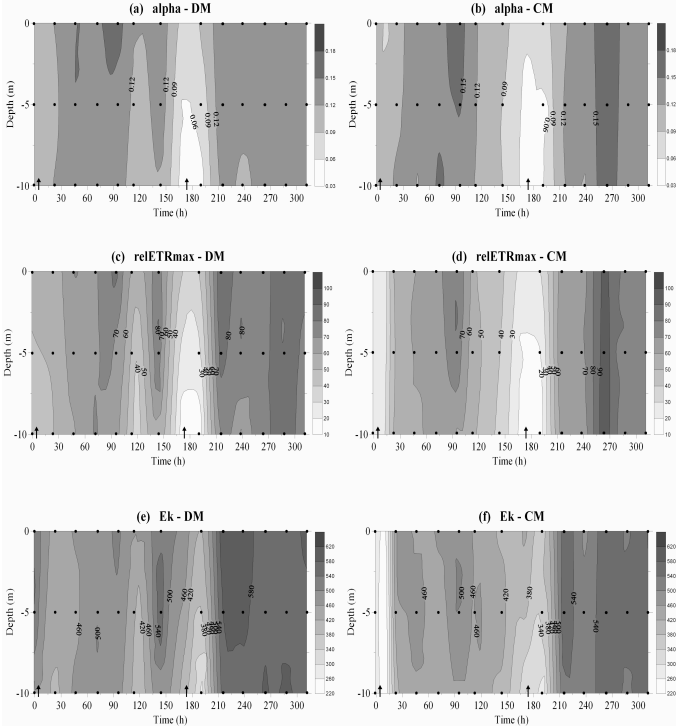

Fig. 6. Evolution of the quantum yield of electron transport ($_{rel}\alpha^{B}$; $\mu mol\,e^{-}\,m^{-2}\,s^{-1}$ [$\mu mol\,photons\,m^{-2}\,s^{-1}$]$^{-1}$) in dust-amended mesocosms (DM; **a**) and control mesocosms (CM; **b**), maximal relative electron transport rate ($_{rel}ETR_{max}$; $\mu mol\,e^{-}\,m^{-2}\,s^{-1}$) in DM **(c)** and CM **(d)**, and light saturation index (Ek; $\mu mol\,photons\,m^{-2}\,s^{-1}$) in DM **(e)** and CM **(f)**, over time (h). The arrows indicate the time at which each dust addition was performed.

BGD
9, 19199–19243, 2012

Assessing the role of dust deposition on phytoplankton ecophysiology

V. Giovagnetti et al.

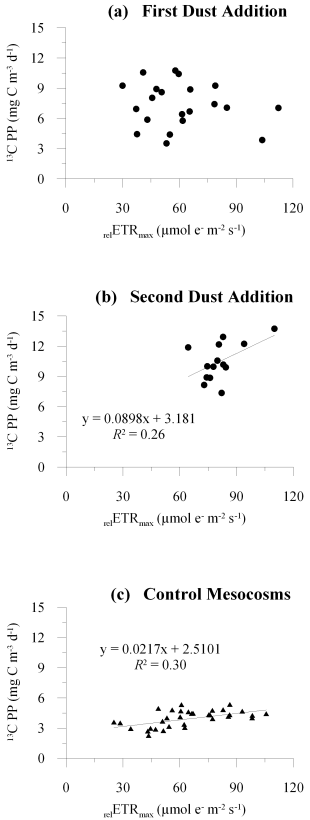

Fig. 7. Relationship between ^{13}C isotopic measurement of net primary production (^{13}C PP; $mg\,C\,m^{-3}\,d^{-1}$) and maximal relative electron transport rate ($_{rel}ETR_{max}$; $\mu mol\,e^{-}\,m^{-2}\,s^{-1}$), during the first (**a**) and the second dust addition (**b**), and during the entire experiment within the control mesocosms **(c)**. The plotted data set represents samples collected at 5 m depth.

BGD
9, 19199–19243, 2012

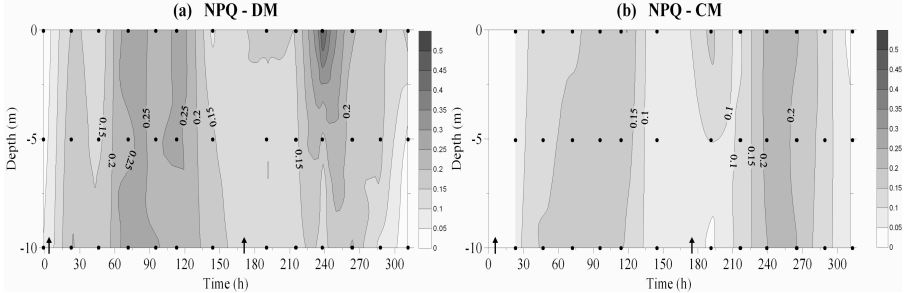

Fig. 8. Evolution of the non-photochemical fluorescence quenching (NPQ) mean values of the phytoplankton community in dust-amended mesocosms (DM; **a**) and control mesocosms (CM; **b**), over time (h). The arrows indicate the time at which each dust addition was performed.

BGD
9, 19199–19243, 2012